

Figure 3. Light ray paths through a fiber.

fiber at the center do so radially (\bar{B} in Figure 3, providing n_r). Thus, the difference in the core-surface birefringence is really the lateral birefringence; i.e.

$$\Delta n_{\text{skin-core}} = (n_{\parallel} - n_{\perp})_{\text{surface}} - (n_{\parallel} - n_{\perp})_{\text{core}} \quad (1)$$

where n_{\parallel} and n_{\perp} refer to indices of refraction relative to the fiber axis. Thus, $\Delta n_{\text{skin-core}}$ is the differential birefringence or the difference in birefringence of the fiber measured at the core or center of the fiber from that measured at the surface. From Figure 3, $n_{\perp s} \equiv n_c$ and $n_{\perp c} \equiv n_r$, and

$$\Delta n_{s/c} = (n_{\parallel s} - n_c) - (n_{\parallel c} - n_r) \quad (2)$$

Assuming n_{\parallel} does not vary with radial position, that is, the limiting case where all the variation in $\Delta n_{s/c}$ is due to lateral birefringence and none to radial variations in n_{\parallel}

$$n_{\parallel s} = n_{\parallel c}$$

and

$$\Delta n_{s/c} = n_r - n_c \equiv \Delta n_{\text{lat}} \quad (3)$$

Direct measurements of lateral birefringence of Kevlar have been made¹ and shown $n_r - n_c \geq 0.020$; however, sample preparation for these measurements is extremely difficult. The results here show $n_r - n_c = 0.026$.

Since $n_r > n_c$ in Kevlar, the plane of the aromatic groups lies radially (C in Figure 3) as opposed to circumferentially. This finding is in accord with Dobbs,⁸ based on measurements using electron microscopy, and Blades,¹ based on measurements of lateral birefringence.

Registry No. Poly(*p*-phenyleneterephthalamide), 24938-64-5; *p*-phenylenediamine-terephthalic acid, 25035-37-4.

References and Notes

- (1) Blades, H. U.S. Patent 3869 430, 1975.
- (2) Pruneda, C. O.; Steele, W. J.; Kershaw, R. P.; Morgan, R. J. *Polym. Prepr., Am. Chem. Soc., Div. Polym. Chem.* **1981**, *22*, 216.
- (3) Chapoy, L. L.; Spaseska, D.; Rasmussen, K.; Dupre, D. B. *Macromolecules* **1979**, *12*, 680.
- (4) Avakian, P.; Blume, R. C.; Gierke, T. D.; Yang, H. H.; Panar, M. *Polym. Prepr., Am. Chem. Soc., Div. Polym. Chem.* **1980**, *21*, 8.
- (5) Simmens, S. C.; Hearle, J. W. S. *J. Polym. Sci., Polym. Phys. Ed.* **1980**, *18*, 871.
- (6) Dobb, M. G.; Hindeleh, A. M.; Johnson, D. J.; Saville, B. P. *Nature (London)* **1975**, *253*, 189.
- (7) Dobb, M. G.; Johnson, D. J.; Saville, B. P. *J. Polym. Sci., Polym. Symp.* **1977**, No. 58, 237.
- (8) Dobb, M. G.; Johnson, D. J.; Saville, B. P. *J. Polym. Sci., Polym. Phys. Ed.* **1977**, *15*, 2201.
- (9) Dobb, M. G.; Johnson, D. J.; Majeed, A.; Saville, B. P. *Polymer* **1979**, *20*, 1284.
- (10) Faust, R. C. *Proc. Phys. Soc. London, Sect. B* **1952**, *65*, 48.
- (11) McLean, J. H. *Text. Res. J.* **1971**, *42*, 36.
- (12) Scott, R. G. *Sci. Tech. Inf.* **1971**, *2*, 36.
- (13) Barakat, N.; El-Hennawi, H. A. *Text. Res. J.* **1971**, *42*, 391.
- (14) Perex, O.; LeCluse, C. *Int. Chem. Dornbirn* **1979**, *20*, 1.
- (15) Hamza, A. A.; Fouda, I. M.; El-Farhatg, K. A.; Badawy, Y. K. *Text. Res. J.* **1980**, *51*, 592.
- (16) Frankfort, H.; Knox, B. U.S. Patent 4134882, 1979.
- (17) Kuhnle, G.; Schollmeyer, E.; Herlinger, H. *Makromol. Chem.* **1977**, *178*, 2725.

Theory of α -Helix-to-Random-Coil Transitions of Two-Chain, Coiled Coils. Application to the T1 and T2 Fragments of α -Tropomyosin

JEFFREY SKOLNICK and ALFRED HOLTZER*

Department of Chemistry, Washington University, St. Louis, Missouri 63130. Received February 16, 1983

In previous papers in this series, an equilibrium statistical mechanical theory is developed and used to fit data for the thermally induced α -helix-to-random-coil transition of two-chain, coiled coils.¹⁻⁴ In that work, application of the theory is made to cross-linked and non-cross-linked α -tropomyosin at both near-neutral³ and acidic pH⁴ and to a synthetic 43-residue peptide made to model salient features of the α -tropomyosin amino acid sequence.^{2,5}

This theory requires as input the amino acid sequence of the polypeptide chain in question and appropriate values, for each amino acid type, of the parameters governing the "short-range" interactions, i.e., the helix initiation (σ) and propagation ($s(T)$) parameters.⁶ The sequence of α -tropomyosin is available.⁷ Algorithms were developed^{4,5} for obtaining $s(T)$ values that reproduce the measurements of that quantity.⁸ Values of σ can be obtained from the same source.⁸ The theory also requires measurements of α -helix content at a known protein concentration. This need was supplied from extant or newly generated circular dichroism data. Recently, the formalism has been extended to include effects of loop entropy, but no data have as yet been treated by this more elaborate theory.⁹

With this input information, the theory, as employed thus far, provides a quantity $-RT \ln w^0$ as a function of temperature.¹⁰ The physical significance of $-RT \ln w^0$ is that it represents Avogadro's number times the change in standard free energy when two widely separated, translationally fixed, α -helical blocks are brought together to form the coiled coil.¹ Thus, it measures the helix-helix interaction in the coiled coil.

Thus far, the theory, although it seems to fit the data, has been employed in a relatively crude manner in that it has been assumed that the value of w^0 depends only on temperature and not on the location of the block within the chain.¹⁻⁴ This use of a site-independent w^0 is suspect since evidence exists from studies of excised fragments of α -tropomyosin that the half of the molecule near the amino end is more stable than near the carboxyl end.¹¹⁻¹³

We report here the results of an investigation of possible site dependence of the helix-helix interaction by application of the theory to two fragments of tropomyosin, T1 and T2.¹¹ These were chosen as particularly apt for our purpose for several reasons: (1) Appropriate thermal denaturation curves, i.e., circular dichroism (usually expressed as mean residue ellipticity $[\theta]$) vs. T , are available and were determined in the same laboratory, which diminishes systematic errors. (2) These two fragments add up to a full tropomyosin molecule but have no residues in common; i.e., they are obtained from the parent chain by a single cut. (3) The cut is almost in the middle of the chain so that each fragment has about the same degree of polymerization. This ensures that certain statistical effects due to chain length are not the source of any observed differences. (4) The stabilities of the T1 and T2 fragments have not been reported to be dependent on the method of isolation, as is the case for some other fragments.¹¹

It will be seen that the theory allows us to compare the two halves of the tropomyosin polypeptide chain with respect to the helix-promoting influence of both the "short-range" interactions and the "long-range" (i.e., helix-helix) interactions.

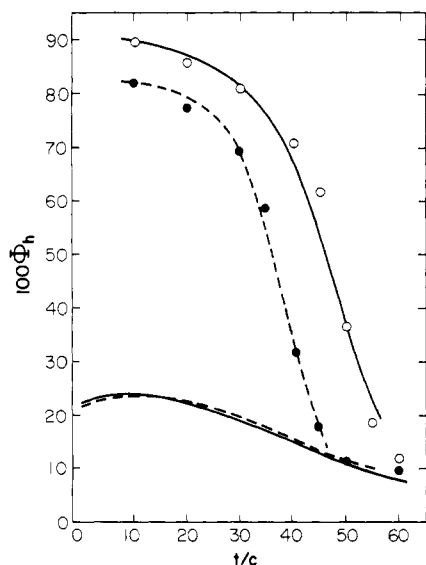


Figure 1. Percent helix ($100\Phi_h$) vs. Celsius temperature for non-cross-linked fragments of α -tropomyosin. Open circles, data for T1 at a concentration of $1.015 \text{ mg}\cdot\text{mL}^{-1}$ ($6.22 \times 10^{-5} \text{ M}$ in chains). Filled circles, data for T2 at a concentration of $0.723 \text{ mg}\cdot\text{mL}^{-1}$ ($4.12 \times 10^{-5} \text{ M}$ in chains). Lower curves are theory for single chains of T1 (full curve) and T2 (dashed curve). Upper curves are theory including algorithmic values of helix-helix interaction as described in text for T1 (solid curve) and T2 (dashed curve).

Methods

Experimental thermal denaturation data for non-cross-linked T1 and T2 fragments were obtained by picking values from the spline curves of $[\Theta]^T/[\Theta]^{10^\circ\text{C}}$ vs. T given in Figure 14 of ref 11. These data were converted to $[\Theta]^T$ values and the concentration of the measurement obtained through additional experimental information supplied by the authors of ref 11. The resulting values of $[\Theta]^T$ were converted to fraction helix as described previously.^{3,4} The experimental data were taken in an aqueous solvent of composition $(\text{KCl})_{100}(\text{KPi})_{50}(\text{DTT})_1(7.0)$.¹⁴ The ionic strength of this medium is somewhat less than that employed previously in the fit of the theory to intact tropomyosin; in the latter case, moreover, the principal cation was Na^+ . However, the helix content is not very dependent on ionic strength and, in any event, our primary purpose here is to compare T1 with T2 rather than either with tropomyosin. The substitution of K^+ for Na^+ is immaterial.

The resulting data of fraction helix vs. T were fit to obtain a theoretical curve of $RT \ln w^0$ vs. T as before, using values in the range 15–90% helix. Fragment T1 has 133 residues, comprising residues 1 (at the amino terminus) through 133 of tropomyosin. It was therefore treated as 19 consecutive, complete heptets, each composed of a 4-block (abcd positions) followed by a 3-block (efg positions). Fragment T2 has 151 residues comprising residues 134–284 of tropomyosin. It was therefore treated as 21 consecutive, complete (4,3) heptets, followed by a single 4-block (abcd positions) at the C terminus.

Results and Discussion

The experimental thermal denaturation data for T1 (open circles) and T2 (filled circles) are shown as percent helix vs. temperature on Figure 1. Since the molar concentrations of T1 and T2 are of the same order of magnitude, the greater relative stability of the amino-terminal segment (T1) is immediately apparent. The upper solid and upper dashed theoretical curves of Figure 1 are discussed below. The lower solid (T1) and lower dashed (T2)

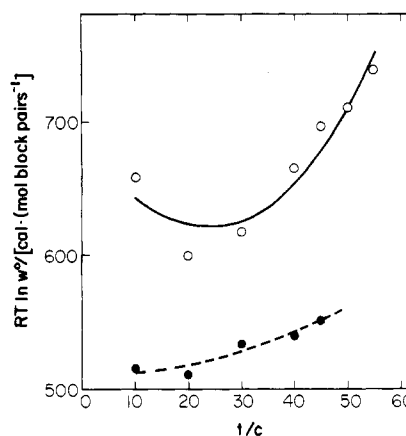


Figure 2. $RT \ln w^0$ vs. Celsius temperature for non-cross-linked fragments of α -tropomyosin. Open circles, values required to fit T1 data; filled circles, values required to fit T2 data. Solid curve is fit to the T1 points. Dashed curve is fit to the T2 points.

theoretical curves of Figure 1 are for single chains ($w^0 = 1$) of the respective fragments. It is immediately evident that the latter two curves are virtually indistinguishable, showing that in spite of the difference in sequence in T1 and T2, the short-range interactions, embodied in the sequence of σ and $s(T)$ values, would lead to essentially the same rather low helix content for single chains of the two segments. It is immediately evident that the theory requires that the observed differences in the two-chain molecules be caused by differences in helix-helix interactions.

This result is stated quantitatively in Figure 2, where values of $RT \ln w^0$ required to fit the data are shown for each fragment. Values for T1 are clearly higher by about $100 \text{ cal}\cdot(\text{mole of block pairs})^{-1}$, indicating greater helix-helix attraction, and are somewhat more temperature dependent. Algorithms chosen to fit values of $RT \ln w^0$ for each fragment are also shown on Figure 2 and when these are used to calculate fraction helix, the resulting curves (shown on Figure 1) for each fragment fit the experimental data rather well.

It should be stressed that the principal conclusion enunciated here, i.e., that the observed advantage in helix stability of the amino half vs. the carboxyl half of the α -tropomyosin molecule is entirely due to helix-helix interaction, follows immediately from the observation that experimentally T1 and T2 differ in helix content at about the same concentration, whereas the theory for single chains predicts they are the same. This conclusion is therefore independent of the validity of the theory as extended to embrace coiled coils. It depends only on the validity of the 2×2 matrix theory for single chains and on the correctness of the input (σ and $s(T)$) parameters employed. The observation that the difference in stability is about $100 \text{ cal}\cdot(\text{mole of block pairs})^{-1}$ does, of course, require use of the coiled coil theory and may be dependent upon its validity. From preliminary work, however, we believe that this observed free energetic difference is about the same when the theory including loop entropy is employed.⁹

Needless to say, the calculations reported here assume site independency for $w^0(T)$ within a given fragment. Thus, the values obtained are perhaps themselves averages over a rather broad range of individual, site-specific interactions. Some data are available for subfragments that could be employed to investigate this question with a finer mesh. However, as noted above, some of the fragments have been observed to have properties dependent upon the method of preparation.¹¹ Furthermore, work is in progress

on the extension of the theory to include the statistical effects of loop entropy⁹ and perhaps also of out-of-register structures (which may exist in the transition zone of the thermal denaturation curve). Under the circumstances, it is wise to wait until a completely self-consistent set of data on the various fragments can be fit with a more complete theory.

Acknowledgment. This study was supported in part by Grant No. GM-20064 from the Division of General Medical Sciences, United States Public Health Service and in part by the Petroleum Research Fund, administered by the American Chemical Society. We also thank the authors of ref 11, Drs. Mary Pato, Alan Mak, and Lawrence Smillie, for graciously supplying us with additional information concerning the experiments reported in that work.

References and Notes

- (1) Skolnick, J.; Holtzer, A. *Macromolecules* **1982**, *15*, 303-314.
- (2) Skolnick, J.; Holtzer, A. *Macromolecules* **1982**, *15*, 812-821.
- (3) Holtzer, M. E.; Holtzer, A.; Skolnick, J. *Macromolecules* **1983**, *16*, 173.
- (4) Holtzer, M. E.; Holtzer, A.; Skolnick, J. *Macromolecules* **1983**, *16*, 462.
- (5) Hodges, R.; Saund, A.; Chong, P.; St-Pierre, S.; Reid, R. *J. Biol. Chem.* **1981**, *256*, 1214-1224.
- (6) For a rather thorough explication of these theoretical ideas and reprints of the benchmark papers, the reader is referred to: Poland, D.; Scheraga, H. "Theory of Helix-Coil Transitions in Biopolymers"; Academic Press: New York, 1970. The particular formulation used here is that of: Zimm, B.; Bragg, J. *J. Chem. Phys.* **1959**, *31*, 526-535.
- (7) Mak, A.; Lewis, W.; Smillie, L. *FEBS Lett.* **1979**, *105*, 232-234.
- (8) Scheraga, H. *Pure Appl. Chem.* **1978**, *50*, 315-324.
- (9) Skolnick, J. *Macromolecules*, in press.
- (10) Some explanation of the notation is required here since the symbol w^0 is now being used in place of the unsuperscripted w employed in ref 1-4. This is to emphasize that the quantity reported in ref 1-4, and here as well, has been obtained by using a theory that leaves loop entropy out of account.
- (11) Pato, M.; Mak, A.; Smillie, L. *J. Biol. Chem.* **1981**, *256*, 593-601.
- (12) Williams, D. L., Jr.; Swenson, C. *Biochemistry* **1981**, *20*, 3856-3864.
- (13) Potekhin, S.; Privalov, P. *J. Mol. Biol.* **1982**, *159*, 519-535.
- (14) We describe complex aqueous solvent media by giving the chemical formula of each solute in parentheses with its millimolarity as subscript, followed by the pH in parentheses. Other abbreviations are as follows: DTT, dithiothreitol; CD, circular dichroism.

Comments on "Effect of Charge Density and Simple Salts on the Diffusion of Polyelectrolytes in Aqueous Solution"¹

KENNETH S. SCHMITZ

Department of Chemistry, University of Missouri—
Kansas City, Kansas City, Missouri 64110.
Received December 2, 1982

Kowblansky and Zema recently reported diffusion coefficients (D_p) for acrylamide/acrylic acid copolymers (PAM) of various charge densities (ζ) as a function of the polymer concentration (C_p) and the added NaBr (C_s).¹ These data suggested that D_p was a linear function of C_p and that the slope (S) and intercept (D_p^0) depended on both ζ and C_s . In particular, D_p^0 decreased and S increased as C_s decreased and/or ζ increased. An apparent peculiar feature of these data when presented on the same graph was a common value for D_p at the polymer concentration $C_p = 0.03\%$ (w/w). This common value of $D_p = 6.4 \times 10^{-8}$ cm²/s led these authors to postulate the existence of a

Table I
Characterization of the Diffusion Data of
Kowblansky and Zema for PAM

C_s , M	$D_p^0 \times 10^8$, cm ² /s	$S \times 10^8$, cm ² /sC(%)	ζ^a
0.1	6.21	13.9	0.02
0.1	5.48	37.2	0.31
0.1	4.66	63.4	0.63
0.1	3.83	101.7	1.85
0.5	6.28	7.2	0.02
0.5	5.79	26.1	0.31
0.5	5.53	31.7	0.63
0.5	4.95	48.5	1.85

^a Defined as $e^2/\epsilon k T b$, where the average interchange spacing b was estimated from potentiometric titration measurements with an assumed value of 2.5 Å between vinyl groups.

"critical concentration" in which "the trends in D_p on either side of the critical point indicate that different interactions dominate above and below this concentration".¹ It is shown in the present note that these linear D_p vs. C_p plots are also consistent with current polyelectrolyte theories without having to propose the existence of a "critical concentration".

For the purpose of quantitative reanalysis of the Kowblansky-Zema data, we employ the expression derived by Schurr et al.^{2,3} for D_p

$$D_p = (1/2)[D_p^0(1 - \Omega) + D_s(1 + \Omega)] \quad (1)$$

where D_p and D_p^0 retain their meaning as above, D_s is the average diffusion coefficient for the counterions and the byions (referred to as the small-ion diffusion coefficient), and

$$\Omega = \frac{D_p^0 - D_s[1 + (2C_s/C_p)Z^{-1}]Z^{-1}}{D_p^0 + D_s[1 + (2C_s/C_p)Z^{-1}]Z^{-1}} \quad (2)$$

where Z is the apparent charge on the polyion. In the dual limits $C_s \gg ZC_p$ and $D_s \gg D_p$, eq 1 reduces to the familiar Donnan equilibrium form

$$D_p = D_p^0[1 + (Z^2 C_p / 2 C_s)] \quad (3)$$

There are two additional effects to be included ad hoc to obtain our operational expression: electrolyte dissipation effects and direct polyion-polyion interactions. The effect of an asymmetric distribution of small ions about the polyion is to provide an additional source of dissipation; hence D_p^0 is expressed in terms of the composite friction factor⁴

$$D_p^0 = kT / \{6\pi\eta a + [(Z^2 e^2 / 12a^2 \epsilon k D_s) \times (1 - ((1 + 2\kappa a) \exp\{-2\kappa a\}))]\} \quad (4)$$

where η is the solvent viscosity, e is the electron charge, a is the polyion radius, κ is the Debye-Hückel screening parameter, and ϵ is the bulk dielectric constant. The quantity in the square brackets is the additional friction due to electrolyte dissipation. Direct polyion-polyion interactions also result in a dependence of D_p on C_p , which we denote by the parameter A_2 . Our final expression for the linear dependence of D_p on C_p is therefore

$$D_p = D_p^0[1 + ((Z^2 / 2C_s) + 2A_2)C_p] \quad (5)$$

where D_p^0 is defined by eq 4. We represent the data of Kowblansky and Zema¹ by the linear expression

$$D_p = D_p^0 + SC(\%) \quad (6)$$

where $C(\%)$ is the percent weight of PAM and D_p^0 is the